

Thermochemistry of Pure-Silica Zeolites

Patrick M. Piccione,[†] Christel Laberty,^{‡,§} Sanyuan Yang,[‡] Miguel A. Cambor,^{||,⊥}
Alexandra Navrotsky,[‡] and Mark E. Davis^{†,*}

Chemical Engineering, California Institute of Technology, Pasadena, California 91125, and Thermochemistry Facility, Department of Chemical Engineering and Materials Science, University of California at Davis, Davis, California 95616

Received: June 13, 2000

A series of pure-silica molecular sieves (structural codes AST, BEA, CFI, CHA, IFR, ISV, ITE, MEL, MFI, MWW, and STT) is investigated by high-temperature drop solution calorimetry using lead borate solvent at 974 K. The enthalpies of transition from quartz at 298 K (in kJ/mol) are AST, 10.9 ± 1.2 ; BEA, 9.3 ± 0.8 ; CFI, 8.8 ± 0.8 ; CHA, 11.4 ± 1.5 ; IFR, 10.0 ± 1.2 ; ISV, 14.4 ± 1.1 ; ITE, 10.1 ± 1.2 ; MEL, 8.2 ± 1.3 ; MFI, 6.8 ± 0.8 ; MWW, 10.4 ± 1.5 ; and STT, 9.2 ± 1.2 . The range of energies observed is quite narrow at only 6.8–14.4 kJ/mol above that of quartz, and these data are consistent with and extend the earlier findings of Petrovic et al.¹ The enthalpy variations are correlated with the following structural parameters: framework density, nonbonded distance between Si atoms, and framework loop configurations. A strong linear correlation between enthalpy and framework density is observed, implying that it is the overall packing quality that determines the relative enthalpies of zeolite frameworks. The presence of internal silanol groups is shown to result in a slight (≤ 2.4 kJ/mol) destabilization of the calcined molecular sieves by comparing calorimetric data for MFI and BEA samples synthesized in hydroxide (containing internal silanol groups) and fluoride (low internal silanol group density) media.

Introduction

During the past decade, interest in new inorganic materials with complex structures and their assembly mechanisms has increased.² An industrially useful class of materials is the zeolites that are porous crystalline aluminosilicates that can act as molecular sieves for shape-selective adsorption and heterogeneous catalysis. These materials can be endowed with strongly acidic or basic sites in the pores by suitable modifications. Pure-SiO₂ zeolites, more properly termed pure-silica molecular sieves, are particularly interesting for practical applications because of their high-temperature stability and hydrophobic nature.³ Despite the industrial importance of zeolites, their syntheses are still not well understood and typically rely on extensive series of trials that use different organocations (structure-directing agents (SDAs)) and conditions to produce new framework structures.^{4–7}

Although purely thermodynamic data cannot answer questions about the kinetics of zeolite syntheses, knowledge of the energetics of different structures provides a framework for rationalizing the driving forces for synthesis, the differences among various structures, and the mechanisms and interactions important in the assembly of these materials.

All silica molecular sieves are metastable with respect to α -quartz, the thermodynamically stable polymorph at ambient conditions. Petrovic et al.¹ obtained calorimetric data for six high-silica molecular sieves (structural codes⁸ FAU, EMT, AFI, MEL, MFI, and MTW; all pure-silica except EMT) and found

them to be energetically higher than quartz by only 7–14 kJ/mol and higher than SiO₂ glass by only 0–7 kJ/mol. They argued that this very modest metastability presented no great hindrance to molecular sieve formation and that the role of the structure-directing agent in hydrothermal syntheses was thus kinetic in nature (selection among configurations that in the pure state would have very similar energetics). Petrovic et al.¹ found no strong correlation between enthalpy (relative to quartz) and structural parameters such as framework density (FD, the number of tetrahedral atoms per nm³). Henson et al.⁹ calculated lattice energies relative to quartz for a collection of 26 structures over a wide range of FD values and found a strong correlation between enthalpy and framework density for their calculated values. They also found a linear correlation between Petrovic's measured values and their calculated ones by ignoring the EMT data point. The work of Petrovic et al.¹ was limited by the variety and quality of materials available a decade ago. Indeed, neither one of their two low-framework density samples (FAU and EMT) was prepared as a pure-SiO₂ material by direct synthesis, and the enthalpy values for these samples cannot be regarded as being as accurate as those for the more dense materials (AFI, MEL, MFI, and MTW). These latter materials, however, cover only a very small range of framework densities (FD = 17.8–19.4 Si atoms/nm³).

To reach more definitive conclusions on the effect of various structural parameters on molecular sieve energetics, experimental thermodynamic data were needed for pure-SiO₂ materials made from direct syntheses and with FDs smaller than 17.8 Si atoms/nm³. Fortunately, in the past few years the use of fluoride instead of hydroxide as the mineralizing agent in zeolite syntheses has enabled the synthesis of pure-SiO₂ materials with

* To whom correspondence should be addressed.

[†] California Institute of Technology.

[‡] University of California at Davis.

[§] Current address: Université Paul Sabatier, 31062 Toulouse, France.

^{||} Instituto de Tecnología Química (CSIC-UPV), 46022 Valencia, Spain.

[⊥] Current address: Industrias Químicas del Ebro, E-50057 Zaragoza, Spain.

lower framework densities (FD = 15.4–17.3 Si atoms/nm³) than those of the materials available to Petrovic et al.¹⁰

The enthalpy for the transition from quartz to molecular sieve, $\Delta H_{\text{trans}}^{298}$, for the pure-SiO₂ molecular sieves AST (all-silica AlPO₄-16), BEA, CHA, IFR (ITQ-4), ISV (ITQ-7), ITE (ITQ-3), MWW(ITQ-1) is determined here in order to obtain thermodynamic data for structures with low FD values. As discussed above, this region of framework density (FD smaller than 17.8 Si atoms/nm³) was hitherto unexplored. Also, the enthalpy for CFI (CIT-5) was measured to determine whether energetics for such a large-pore structure follow the trends seen for samples with smaller pore sizes; it was long believed that extra-large-pore materials were hard to synthesize because of thermodynamic instability. Enthalpies for MFI and BEA samples synthesized in both fluoride and hydroxide media were investigated as well. Although the fluoride materials are essentially free of internal silanol defects, the hydroxide materials contain such defects and are more typical of those used for industrial applications. From these samples, an estimate of the defect energetics can be obtained.

High-temperature drop solution calorimetry using lead borate solvent at 974 K is employed here to measure enthalpies of transformation from quartz with a standard error of ± 1 to ± 2 kJ/mol. The results and their implications with regard to the stability of the different frameworks, the correlations with framework structural features, and comparisons with previously reported trends are presented.

Experimental Section

Samples. Unless noted otherwise, the SiO₂ source for the synthesis of all molecular sieves was tetraethoxysilane (TEOS). For BEA/F and BEA/OH, the complete reaction mixture was formulated to the compositions specified below and the TEOS was completely hydrolyzed before heating the synthesis gel. The ethanol generated by hydrolysis was removed by evaporation at room temperature. For AST, CFI, CHA, IFR, ISV, and STT, the reaction mixture omitting HF was formulated to the compositions specified below and the TEOS was completely hydrolyzed before heating the synthesis gel. The ethanol generated by hydrolysis was removed by evaporation at room temperature, and the HF was added to the correct composition.

AST. The *tert*-butyltrimethylammonium (TBTMA)-mediated synthesis of pure-SiO₂ AST used a gel composition of 1 SiO₂/0.5 TBTMAF/13 H₂O.¹² After reaction at 423 K and autogenous pressure for 6 days in a Teflon-lined stainless steel reactor that was rotated at 60 rpm, the product was collected by cooling the mixture to room temperature, filtering, and washing with water and then acetone. The sample was calcined four times in air at 1223 K for 3 h to remove the occluded organics.

BEA/F. The TEAF-mediated synthesis of pure-SiO₂ zeolite β employed a reaction composition of 1 SiO₂/0.5 TEAF/7.25 H₂O.¹³ In this synthesis, two rotary evaporations were performed to remove the ethanol formed by hydrolysis. The synthesis was conducted at 413 K and autogenous pressure for 14 days in a Teflon-lined stainless steel reactor, and the products were collected by cooling the mixture to room temperature, filtering, and washing with water and then acetone. The sample was calcined at 823 K in air for 6 h to remove the occluded organics. This sample will be denoted here as BEA/F to distinguish it from the hydroxide-mediated sample of zeolite β .

BEA/OH. For the trimethylenebis(*N*-methyl,*N*-benzyl)piperidinium) hydroxide-mediated synthesis of pure-SiO₂ BEA (BEA/OH), the gel composition was 1 SiO₂/0.10 R(OH)₂/35 H₂O, where R is trimethylenebis(*N*-methyl,*N*-benzyl)piperidinium),

synthesized as described previously.¹⁴ After reaction at 408 K and autogenous pressure for 9 days in a Teflon-lined stainless steel reactor, the products were collected by cooling the mixture to room temperature, filtering, and washing with water and then acetone. The sample was calcined in air at 873 K for 8 h to remove the occluded organics.

CFI. A sample of pure-SiO₂ CFI was prepared from a gel composition of 1 SiO₂/0.50 TOH/0.50 HF/15 H₂O, where T is the *N*-methyl(-)-sparteinium cation.¹⁵ After reaction at 448 K and autogenous pressure for 4 days in a Teflon-lined stainless steel reactor with rotation at 60 rpm, the product was collected by cooling the mixture to room temperature, filtering, and washing with water and then acetone. The sample was calcined in air at 923 K for 3 h to remove the occluded organics.

CHA. For the *N,N,N*-trimethyladamantammonium-mediated synthesis of pure-SiO₂ CHA, the gel composition was 1 SiO₂/0.5 TMAdaF/3 H₂O, where TMAda is *N,N,N*-trimethyladamantammonium.¹⁶ After reaction at 423 K and autogenous pressure for 40 h in a Teflon-lined stainless steel reactor that was rotated at 60 rpm, the products were collected by cooling to room temperature, filtering, and washing with water and then acetone. The sample was calcined at 853 K for 3 h in air to remove the occluded organics.

IFR. The *N*-benzyl-1-azoniumbicyclo[2,2,2]-octane-mediated synthesis of pure-SiO₂ IFR utilized the gel composition 1 SiO₂/0.50 C₁₄H₂₀N⁺OH⁻/0.50 HF/15 H₂O, where C₁₄H₂₀N⁺ is *N*-benzyl-1-azoniumbicyclo[2,2,2]-octane.¹⁷ After reaction at 423 K and autogenous pressure for 12 days in a Teflon-lined stainless steel reactor rotating at 60 rpm, the products were collected by cooling to room temperature, filtering, and washing with water and then acetone. The sample was calcined at 923 K for 3 h in air to remove the occluded organics.

ISV. A sample of pure-SiO₂ ISV was prepared from a gel composition of 1 SiO₂/3 C₁₄H₂₆NOH/3 HF/1 H₂O, where C₁₄H₂₆N⁺ is 1,3,3-trimethyl-6-azoniumtricyclo[3.2.1.4^{6,6}]dodecane.¹⁸ After reaction at 423 K and autogenous pressure for 15 days in a Teflon-lined stainless steel reactor rotating at 60 rpm, the products were collected by cooling to room temperature, filtering, and washing with water and then acetone. The sample was calcined in air at 853 K to remove the occluded organics.

ITE. Pure-SiO₂ ITE was prepared from a gel composition of 1 SiO₂/0.5 C₁₂H₂₄NOH/0.5 HF/7.7 H₂O, where C₁₂H₂₄N⁺ is 1,3,3,6,6-pentamethyl-6-azoniabicyclo[3.2.1]octane.¹⁹ After reaction at 423 K and autogenous pressure for 19 days in a Teflon-lined stainless steel reactor rotating at 60 rpm, the products were collected by cooling to room temperature, filtering, and washing with water. The sample was calcined in air at 853 K to remove the occluded organics.

MEL. Pure-SiO₂ MEL was produced from a gel of composition 1 SiO₂/0.25 ROH/0.05 KOH/18 H₂O, where R is *N,N*-diethyl-3,5-dimethylpiperidinium.¹¹ The silica source for this synthesis was Cab-O-Sil M-5. After reaction at 443 K in a rotating Teflon-lined stainless steel reactor, the product was collected by cooling the mixture to room temperature, filtering, and washing with water and then acetone. The sample was calcined in air at 873 K to remove the occluded organics.

MFI/F. For the TPA-mediated synthesis of pure-SiO₂ MFI in fluoride media (denoted MFI/F), the gel composition was 1 SiO₂/0.44 TPAOH/0.5 HF/50 H₂O. The silica source for this synthesis was Cab-O-Sil M-5. After reaction at 448 K and autogenous pressure for 5 days in a Teflon-lined stainless steel reactor, the products were collected by cooling to room temperature, filtering, and washing with water and then acetone.

The sample was calcined in air at 823 K for 6 h to remove the occluded organics.

MFI/OH. A sample of pure-SiO₂ MFI made with hydroxide as the mineralizer (denoted MFI/OH) was prepared from a gel of composition 1 SiO₂/0.1 TPABr/0.5 C₄H₁₀N₂/50 H₂O, where C₄H₁₀N₂ is piperazine. The silica source for this synthesis was Cab-O-Sil M-5. The gel was seeded with 0.6% MFI which had been previously prepared with tetrapropylammonium (TPA) ions as the SDA. After reaction at 423 K and autogenous pressure for 8 days in a Teflon-lined stainless steel reactor, the products were collected by cooling to room temperature, filtering, and washing with water and then acetone. The sample was calcined in air at 823 K for 7 h to remove the occluded organics.

MWW. Pure-SiO₂ MWW was made from a gel of composition 1 SiO₂/0.25 TMAdaOH/0.40 HMI/44 H₂O, where TMAda is *N,N,N*-trimethyl-1-adamantammonium and HMI is hexamethyleneimine.²⁰ The silica source for this synthesis was Aerosil 200. After reaction at 423 K and autogenous pressure for 17 days in a Teflon-lined stainless steel reactor rotating at 60 rpm, the products were collected by cooling to room temperature, filtering, and washing with water and then acetone. The as-made sample was calcined in air at 853 K to remove the occluded organics and to produce the fully connected three-dimensional framework.²⁰

STT. For the TMAda⁺-mediated synthesis of pure-SiO₂ STT, the gel composition was 1 SiO₂/0.50 TMAdaOH/0.50 HF/15 H₂O.²¹ After reaction at 423 K and autogenous pressure for 30 days in a Teflon-lined stainless steel reactor, the products were collected by cooling to room temperature, filtering, and washing with water and then acetone. The sample was calcined in air at 853 K for 3 h to remove the occluded organics.

Before calorimetry, the samples were pressed into ~15 mg pellets and dried in air overnight at 473 or 573 K to remove most of the absorbed water. All sample pellets were stored in an Ar-filled glovebox prior to calorimetry.

Characterizations. Powder X-ray diffraction (XRD) patterns were collected at room temperature on a Scintag XDS 2000 diffractometer (liquid nitrogen cooled Ge detector, Cu K α radiation, $\lambda = 1.54184 \text{ \AA}$) operating in a Bragg-Bretano geometry. The data were obtained in a stepwise mode with 2θ ranging from 2 to 51° (step size = 0.01°, count time = 4 s) in order to identify the crystalline phases present before and after drying. Thermogravimetric analyses (TGA) were performed on 35–50 mg samples using a Netzsch STA409 system to measure the mass fraction of water present in the samples introduced into the calorimeter. The heating rate was 10 K/min to 1473 K, and dry Ar was used as the carrier gas to avoid sample rehydration. Buoyancy corrections were performed for all runs by allowing the sample to cool to room temperature and heating it back to 1473 K. Alternatively, the measurement was performed on approximately 15 mg samples using a Dupont 2100 instrument. The heating rate was 10 K/min to 1173 K, and the buoyancy correction was based on a run with 15 mg Pt.

Solid-state ²⁹Si NMR spectra for the BEA/OH and MFI/OH samples were collected on a Bruker AM300 spectrometer equipped with a Bruker cross-polarization, magic angle spinning (MAS) accessory. The samples were packed into 7 mm ZrO₂ rotors and spun in air at 4 kHz. Proton-decoupled ²⁹Si NMR spectra (59.63 MHz) referenced to tetrakis(trimethylsilyl)silane (downfield peak at $\delta = -10.053 \text{ ppm}$) were collected using MAS. The results were analyzed with the Tecmag MacFID software; simulations using Gaussian lines were carried out to estimate the defect density (Q₃/Q₄ ratio).

The adsorption capacity of the BEA/OH sample for cyclohexane was measured at room temperature using a McBain–Bakr balance. The C₆H₁₂ vapor was delivered from the liquid phase. The microporous volume was determined at a relative vapor pressure P/P_0 of 0.33. Prior to the adsorption experiment, the sample was dehydrated at 473 K under a vacuum of 10⁻³ Torr for 2 h. The adsorption capacity is reported in milliliters of liquid per gram of dry zeolite, assuming bulk liquid density for the adsorbate in the micropores.

Calorimetry. Drop solution calorimetry was employed to obtain the heats of solution of the molecular sieves. In each experiment, the sample pellet was dropped from room temperature into the molten 2PbO·B₂O₃ solvent in the calorimeter at 973 K. SiO₂ is well-known to be soluble in lead borate, so the same final state is obtained for all molecular sieves upon dissolution.¹ A quartz sample (Fluka, 99.5%) was used in addition to the molecular sieves so that the enthalpy for the transition quartz (298 K) → molecular sieve (298 K), $\Delta H_{\text{trans}}^{298}$, could be obtained by difference. All thermochemical measurements were performed using a Tian–Calvet twin microcalorimeter that has been described in detail elsewhere,²² operating under flowing Ar to assist in the removal of any water vapor. The calibration factor for the calorimeter (J/ μV) was obtained by dropping ~15 mg pellets of alumina (Aldrich, 99.99%) stabilized in the corundum phase by heating overnight at 1773 K. The overall methodology is now standard and has been described previously.^{1,23,24}

Results

Characterization. The X-ray powder diffraction (XRD) patterns indicated the presence of a single molecular sieve phase for each sample. All powder patterns except for BEA/OH displayed sharp peaks and were in excellent agreement with published data (AST,¹² BEA,¹³ CFI,²⁵ CHA,¹⁶ IFR,¹⁷ ISV,¹⁸ ITE,¹⁹ MEL,²⁶ MFI,²⁷ MWW,²⁰ and STT²⁸). For the BEA/OH sample, repeated attempts to completely remove the large, bulky organic SDA without degrading the XRD pattern (e.g., calcinations at lower temperature, extractions) were unsuccessful. This is a common problem for pure-silica zeolite β prepared in hydroxide media. To quantify the degree of structural damage, cyclohexane adsorption was performed on the BEA/OH sample calcined in air at 873 K. The adsorption capacity for cyclohexane with this material was found to be 0.24 mL/g and compares favorably to literature data.²⁹ Thus, the structure is not significantly collapsed by the calcination procedure.

For all materials other than BEA/OH, the crystal sizes were larger than 1 μm . For particles larger than 1 μm , surface energy effects do not significantly affect the measured energetics;¹ hence, they were neglected in this work.

The TGA results are shown in Table 1, along with the calculated molar mass (per mol SiO₂) and water contents. The amount of water present in the dehydrated samples was calculated by taking the difference of the mass losses at 1373 or 1073 K and at the dehydration temperature of 473 or 573 K. The water contents are typically below 1% for all the materials synthesized in fluoride media, indicating successful dehydration. These water contents are nonzero, however, because only a partial dehydration is carried out by heating to 473–573 K; treatment at higher temperatures could have achieved complete dehydration, but with the possible risk of damaging the molecular sieve frameworks, at least for the hydroxide-mediated samples. Two of the materials synthesized using hydroxide ions as the mineralizer (BEA/OH and MWW) contain slightly larger amounts of water (0.5–2.0%) as expected due to the hydrophilic

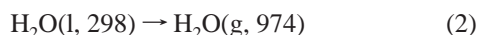
TABLE 1: Results from Thermogravimetric Analysis of Silica Materials

sample	% mass loss TGA (wt)	mol H ₂ O per mole SiO ₂	MW per mole SiO ₂
quartz	0.27	0.009	60.25
MEL	0.38	0.013	60.31
MWW	1.8	0.061	61.19
IFR	0.55	0.018	60.42
ITE	0.42	0.014	60.34
AST	0.39	0.013	60.32
STT	0.42	0.014	60.34
CHA	0.66	0.022	60.48
BEA/F	0.12	0.004	60.16
MFI/F	0.06	0.002	60.12
CFI	0.59	0.020	60.44
ISV	0.05	0.002	60.12
BEA/OH	0.93	0.031	60.65
MFI/OH	0.37	0.012	60.31

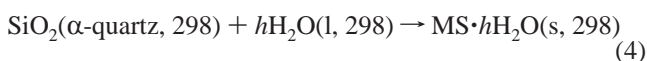
nature of their defect sites (see below). The calorimetry experiments with MWW were performed on the air-exposed material because the mechanical properties of the pellets prepared from the oven-dried material were poor and the pellets could not be made to retain their shape. This fact further explains the high (1.8%) amount of water in this material.

The ²⁹Si solid-state NMR spectra of the MFI/OH and BEA/OH samples confirmed the presence of Q₃ (defect) Si sites in both samples (peak below -105 ppm). A quantitative deconvolution into Gaussian line shapes carried out with the MacFID software gave Q₃/Q₄ ratios of 0.43 for BEA/OH and 0.041 for MFI/OH. The corresponding percentages of silicon present as Q₃, denoted here as Si_d, are Si_d = 29.9% (BEA/OH) and 4.0% (MFI/OH). The unusually low defect site density for the MFI/OH sample is undoubtedly due to the use of piperazine as the SDA. The mass losses corresponding to complete annealing of the defect sites calculated from these Si_d values are 0.37% and 0.02%, respectively. Because the TGA mass losses are composed of both (possibly incomplete) annealing and the loss of water bound in molecular form, the TGA losses are expected to be higher than those calculated from the ²⁹Si NMR data. Indeed, the TGA mass losses for the BEA/OH and MFI/OH are 0.93% and 0.37%, respectively, so the ²⁹Si NMR and TGA data are consistent.

Enthalpies of Transition (Quartz → Molecular Sieve), $\Delta H_{\text{trans}}^{298}$. The enthalpies of transition for the reaction quartz → molecular sieve at 298 K were calculated by taking the difference between the heats of drop solution for quartz and the molecular sieve. The following thermodynamic cycle was used to determine the energetics of the molecular sieve frameworks, where MS is a generic designation for any of the molecular sieve frameworks and *h* is the number of moles of water present per mole of SiO₂:



By addition of these equations, $\Delta H_{\text{trans}}^{298}$ for the formation of MS from α -quartz is obtained:



where $\Delta H_4 = \Delta H_1 + h\Delta H_2 + \Delta H_3 = \Delta H_{\text{trans}}^{298}$.

The enthalpies ΔH_1 and ΔH_3 are the experimentally measured heats of drop solution for the molecular sieves and quartz, respectively; ΔH_2 was obtained from a linear interpolation of the water enthalpies at 900 and 1000 K to 974 K (from ref 30), giving 70.85 kJ/mol H₂O. The ΔH_2 contribution to the overall transition enthalpy represents the heat required to completely vaporize and heat the residual amount of water in the dehydrated molecular sieves from 298 K to the calorimeter operating temperature of 974 K. This correction assumes that the residual H₂O present is energetically the same as liquid water; that is, any enthalpy of hydration of the framework is neglected. Hu et al.³¹ measured enthalpies of hydration for microporous AlPO₄ materials and reported values of -12 kJ/mol relative to liquid water. The pure-SiO₂ molecular sieves are more hydrophobic than the aluminum phosphates. Therefore, it is likely that they interact less favorably with water, leading to enthalpies of hydration less negative than -12 kJ/mol. Indeed, the enthalpy of hydration for pure-silica defect-free zeolite BEA has been shown to be small compared to the heat of vaporization of water,³² and this is expected to be true for all defect-free hydrophobic samples. To estimate the impact of nonzero hydration energetics on the $\Delta H_{\text{trans}}^{298}$, enthalpy of transition values assuming both an enthalpy of hydration of -10 kJ/mol (slightly less exothermic than the value for the AlPO₄ materials) and an enthalpy of hydration of 10 kJ/mol (an endothermic, physically unreasonable overestimate) were calculated in addition to the $\Delta H_{\text{trans}}^{298}$ values derived from a zero enthalpy of hydration.

Measured calorimetric data and calculated enthalpies of transition are shown in Tables 2 and 3. Table 3 lists the transition enthalpy $\Delta H_{\text{trans}}^{298}$ for each molecular sieve with the associated standard error that includes and neglects the ± 10 kJ/mol hydration enthalpies as discussed above. The 95% confidence intervals were calculated as

$$\sigma_{95} = \frac{1.96}{N-1} [\sigma_1^2 + \sigma_3^2 + (10h)^2 + 0.7^2]^{1/2}$$

where σ_1 and σ_3 are the standard deviations for ΔH_1 and ΔH_3 , respectively, and the third and fourth terms account for the uncertainty in the nonzero water interaction energy (± 10 kJ/mol) and TGA mass loss, respectively. An uncertainty of approximately 0.7 kJ/mol due to TGA errors was calculated by a propagation-of-errors approach assuming an estimated mass loss uncertainty of $\pm 0.3\%$. *N* is the number of drop solution measurements for each sample.

Discussion

Enthalpies of Transition, $\Delta H_{\text{trans}}^{298}$. The measured drop solution enthalpies for quartz are within experimental error of the previous value³³ of 39.1 ± 0.3 kJ/mol. Furthermore, the measured value for MEL (8.2 ± 1.3 kJ/mol) is in good agreement with the previously measured value of 8.2 ± 1.0 kJ/mol.¹ Because the measured $\Delta H_{\text{trans}}^{298}$ values of MEL and MFI/OH are essentially identical (8.2 and 8.0 kJ/mol), the presence¹¹ of MFI intergrowths in the previously synthesized MEL sample cannot have significantly affected the reported enthalpy.¹ The MFI/F value of 6.8 ± 0.8 kJ/mol is also close to the previously reported value of 8.2 ± 0.8 kJ/mol.¹ The range of $\Delta H_{\text{trans}}^{298}$ values for the molecular sieves studied here is 6.8–14.4 kJ/mol, in good accord with a similar range (7–14 kJ/mol) reported by Petrovic et al.¹ The uncertainty in $\Delta H_{\text{trans}}^{298}$ is 1–1.5 kJ/mol, typical of this class of calorimetry experiments.²²

TABLE 2: Measured Calorimetric Data

sample	$\Delta H_{\text{dropsol}}$ (J/mg)	std dev (J/mg)	no. of data points	error (J/mg) ^a	$\Delta H_{\text{dropsol}}$ uncorrected (kJ/mol SiO ₂)	$\Delta H_{\text{dropsol}}$ (kJ/mol SiO ₂) ^a
quartz	0.6765	0.0199	9	0.0138	40.76	0.83
MEL	0.5442	0.0144	6	0.0126	32.82	0.76
MWW	0.5561	0.0104	4	0.0118	34.03	0.72
IFR	0.5194	0.0054	4	0.0061	31.38	0.37
ITE	0.5144	0.0092	6	0.0081	31.04	0.49
AST	0.5005	0.0078	6	0.0069	30.19	0.41
STT	0.5291	0.0098	6	0.0086	31.93	0.52
CHA	0.5003	0.0163	5	0.0159	30.26	0.96
BEA/F	0.4921	0.0056	7	0.0045	29.60	0.27
MFI/F	0.5317	0.0034	6	0.0030	31.96	0.18
CFI	0.5160	0.0031	7	0.0025	31.19	0.15
ISV	0.4170	0.0144	7	0.0116	25.07	0.69
BEA/OH	0.4808	0.0060	8	0.0044	29.16	0.27
MFI/OH	0.5219	0.0046	7	0.0037	31.48	0.22

^a 95% confidence interval.**TABLE 3: Calculated Calorimetric Data (All Data in kJ/mol SiO₂)**

sample	water correction	$\Delta H_{\text{dropsol}}$ corrected	$\Delta H_{\text{trans}}^{298}$	$\Delta H_{\text{trans}}^{298 a}$	with 10 kJ/mol hydration		with -10 kJ/mol hydration	
					$\Delta H_{\text{dropsol}}$ corrected	$\Delta H_{\text{trans}}^{298}$	$\Delta H_{\text{dropsol}}$ corrected	$\Delta H_{\text{trans}}^{298}$
quartz	0.64	40.12	0.00	N/A	40.21	0.00	40.03	0.00
MEL	0.90	31.92	8.19	1.34	32.05	8.16	31.80	8.23
MWW	4.33	29.70	10.42	1.45	30.31	9.90	29.08	10.94
IFR	1.31	30.08	10.04	1.17	30.26	9.95	29.89	10.14
ITE	1.00	30.04	10.08	1.21	30.18	10.03	29.90	10.13
AST	0.93	29.26	10.86	1.18	29.39	10.82	29.13	10.90
STT	1.00	30.93	9.19	1.22	31.07	9.14	30.79	9.24
CHA	1.57	28.69	11.43	1.47	28.91	11.30	28.47	11.56
BEA/F	0.28	29.32	9.29	0.82	29.36	9.25	29.28	9.33
MFI/F	0.14	31.82	6.78	0.80	31.84	6.76	31.80	6.80
CFI	1.40	29.79	8.82	0.81	29.98	8.62	29.59	9.02
ISV	0.13	24.94	14.37	1.07	24.96	14.36	24.92	14.39
BEA/OH	2.22	26.94	11.67	0.88	27.25	11.35	26.63	11.98
MFI/OH	0.88	30.60	8.01	0.82	30.72	7.88	30.48	8.13

^a 95% confidence interval.

The contribution of the water vaporization to the enthalpies ($h\Delta H_2$) is below 1.6 kJ/mol for all samples synthesized in fluoride media because they contain less than 0.6% water. For the fluoride samples, the water contribution amounts to no more than 20% of the total enthalpy measured. For the samples synthesized in hydroxide media, the water correction takes on generally higher values because the solids contain more water. For MEL and MFI/OH, this correction is only 0.87 kJ/mol, but for MWW and BEA/OH the corrections are 4 kJ/mol. The enthalpies of these last two samples, therefore, are somewhat more uncertain than the other enthalpies reported here.

The $\Delta H_{\text{trans}}^{298}$ values calculated with ± 10 kJ/mol hydration enthalpies do not differ significantly from the $\Delta H_{\text{trans}}^{298}$ values that ignore this contribution (see Table 3); the discrepancy is less than 0.2 kJ/mol for all fluoride-synthesized samples. For the hydroxide-synthesized samples, the discrepancy is larger (up to 0.5 kJ/mol for MWW) but still well within the reported uncertainties. The assumption that the water behaves as liquid water, therefore, does not significantly impact the final enthalpy values and trends. For the remainder of these discussions, the values calculated assuming that the physically adsorbed water behaves as bulk liquid water will be used. The data for BEA/F and MFI/F must be considered the most accurate determination of the BEA and MFI framework enthalpies because they consist of a SiO₂ framework with very low silanol defect densities. For further discussion, see Defect Energetics below. Before a closer study of the correlation between structure and energetics, some general remarks are in order.

This study focuses on determining $\Delta H_{\text{trans}}^{298}$ for a set of molecular sieves with significantly different frameworks (lower density for pure-SiO₂ materials, larger and different ring sizes) than those examined in earlier studies.¹ Notwithstanding this wider range of structural features, the enthalpies of the molecular sieves studied here still fall within the same narrow range of enthalpies of 6.8–14.4 kJ/mol less stable than that of quartz. Pure-silica molecular sieves are therefore energetically quite close to quartz. This is also true for CFI which, despite its pores of 14-membered rings, has an enthalpy only 8.8 kJ above that of quartz. The enthalpy for STT also falls in this range and shows that frameworks composed of seven- and nine-membered rings (7-MR and 9-MR), extremely rare in zeolites and found only in STT among pure-silica materials, do not display unusual energetics. Thus, there appears to be nothing intrinsically unstable in frameworks containing 7-MR and 9-MR despite their scarcity among zeolites. The same conclusion has been reached from lattice energy minimizations of the STT structure using the program GULP,³⁴ although the calculated enthalpy of STT relative to quartz (13.85 kJ/mol) was larger than the experimental one.²⁸ The systematic tendency of the GULP calculations to overestimate pure-silica molecular sieve enthalpies was already evident in the early work by Henson et al.⁹ Most SiO₂ molecular sieves currently known have structural features (pore sizes and framework densities) that fall within the range of those of molecular sieves for which the enthalpies have now been determined.^{1,8} We conclude that $\Delta H_{\text{trans}}^{298}$ values for all SiO₂

molecular sieves presently known can be expected to lie within a narrow region at approximately 6.8–14.4 kJ/mol less stable than quartz.

Defect Energetics. A comparison of the $\Delta H_{\text{trans}}^{298}$ values for the samples of MFI and BEA synthesized in both hydroxide and fluoride media gives higher values for the hydroxide samples. Despite the limited number of data points available, the presence of silanol defects is shown to have a slight destabilizing effect (1.2 kJ/mol for MFI and 2.4 kJ/mol for BEA). Because zeolite BEA is well-known to have the largest number of defects of all pure-silica molecular sieves, these results place an upper bound of 2.4 kJ/mol on the energetic effect of the defects for any crystalline silica phase. This value is smaller than the observed total range of enthalpies for the silica molecular sieves, so for these materials the presence of defects does not significantly alter the relative energetics of the various frameworks.

Finally, note that among pure-SiO₂ molecular sieves prepared in hydroxide media, BEA is known to contain the largest number of defect sites, so the MEL and MWW $\Delta H_{\text{trans}}^{298}$ values are assumed to be good indications of the corresponding idealized framework enthalpies despite the fact that the samples were synthesized in the presence of OH⁻ ions. MWW, in particular, is known to have a large concentration of defects in the as-made layered form, but the large majority of these anneal upon calcination to produce the 3-D framework.²⁰

Implications for Zeolite Synthesis. The $\Delta H_{\text{trans}}^{298}$ values of pure-silica molecular sieves are shown here to be 6.8–14.4 kJ less stable than that of quartz. The enthalpies of amorphous silicas derived from gels lie in the same energetic region as the molecular sieve enthalpies (the former are 0–10 kJ/mol less stable^{35,36} than silica glass, which is itself 9.1 kJ/mol less stable than quartz³¹), so the formation of pure-SiO₂ molecular sieves from amorphous precursors is not appreciably hindered on enthalpy grounds. In fact, for the most stable molecular sieves ($\Delta H_{\text{trans}}^{298} \leq 9.1$ kJ/mol), the amorphous \rightarrow molecular sieve transformation is even exothermic by at least 0–2.5 kJ/mol. The entropies of the amorphous species, however, are necessarily higher than those of the crystalline *ordered* molecular sieves, so whether ΔG will favor the amorphous or crystalline phases is not certain. In any event, the magnitude of ΔG for the amorphous \rightarrow molecular sieve transformation is clearly quite small. Because the available thermal energy at the typical synthesis temperature of 373 K is $RT = 3.1$ kJ/mol, all pure-SiO₂ molecular sieve frameworks are within twice the available thermal energy ($2RT = 6.2$ kJ/mol) of each other and are not significantly less stable than quartz. Further, even mesoporous silicas such as the MCM-41 materials have been shown to be no more than 14–15 kJ/mol less stable than quartz. Thus, they must be considered to lie in the same general enthalpy region even though their pore sizes and molar volumes are several times larger than those of even the most porous molecular sieve.³⁷ Therefore, there are no large thermodynamic barriers to the interconversions among the many polymorphs of SiO₂.

The narrowness of the enthalpy range covered by different frameworks undoubtedly explains the multiplicity (around 30) of known SiO₂ polymorphs.⁸ Indeed, similar energetics are expected for other isocompositional classes of dehydrated microporous materials, for example, the AlPO₄ materials.³¹ The role of the structure-directing agent cannot then be to help stabilize otherwise very unstable structures but rather to form organic–inorganic composites that select one set of structures over another. The presumably exothermic nature of the interaction to form such organic–inorganic composites can be invoked

to explain the preferential formation of ordered porous frameworks over amorphous silicas in molecular sieve syntheses, even though the amorphous silicas would be expected to be favored on entropic grounds.

More instructively, perhaps, the self-assembly of the various silica polymorphs can be understood by considering the organic species present in the synthesis gel or solution. These organic species participate in three essentially different types of interactions: organic–organic (O–O), organic–inorganic (O–I), and organic–water (O–W) interactions. The relative strengths of these three interactions presumably determine the kind of structure that the self-assembly process will yield. If sufficiently strong O–O attractive interactions are present, organized organic structures are formed. These structures, in turn, may be able to organize the water and silicate species around themselves, leading to structures with large pores due to the relatively large size of the O–O aggregates. A typical example is the synthesis of mesoporous materials using surfactants as the SDAs. If the O–I interactions predominate, precursors to molecular sieves with the organic and inorganic species in intimate contact can form. In this case, crystalline materials can result after self-assembly; because of the intimate O–I contact, they are typically porous (i.e., they are molecular sieves). If neither O–O nor O–I interaction is sufficiently strong to lead to ordered structures, there is no opportunity to form either micelles or precursors to molecular sieves. In such cases, either amorphous or dense materials are synthesized, probably depending in large part on the general conditions (pH, temperature, silica concentration, and synthesis time). A schematic representation of these various processes is shown in Figure 1.

Relationship between Structure and Energetics. Previous studies reported no strong correlation between enthalpies and framework structure. Petrovic et al. attempted to correlate enthalpies of formation with both framework density and mean Si–O–Si angle without success.¹ Ab initio calculations³⁸ suggest that although large Si–O–Si angles (for reference, the angle is 143.6° for quartz, whereas it ranges from 132 to 179° for molecular sieves) do not appreciably destabilize these structures, angles below about 135° will do so. A weak correlation between the overall enthalpy and the fraction of Si–O–Si angles below 140° was indeed found by Petrovic et al.¹ by ignoring the data for the dense phases that did not fit within the trend. As discussed above, these findings suffered from the relative narrowness of the density range for which pure-silica molecular sieves could be prepared. The later work by Henson et al.⁹ reanalyzed the experimental values of Petrovic et al.¹ and concluded that after ignoring the EMT data point, they showed a dependence of $\Delta H_{\text{trans}}^{298}$ on the framework density. Henson et al.⁹ presented theoretical calculations for additional structures that confirmed this trend. Having more than doubled the number of molecular sieves for which experimental $\Delta H_{\text{trans}}^{298}$ values are available, we are now in a better position to determine how well the enthalpies and FDs correlate. The FD values considered in this paper are those derived from the structural data available for the calcined silica materials. These values may differ significantly from the values collected in ref 8 (corresponding to the “Type Materials”, which frequently are high-alumina zeolites or aluminophosphates) or from the FD_{Si} values in ref 8 (derived from the DLS-minimized silica structure).

The structural and thermodynamic data for all tetrahedrally coordinated SiO₂ polymorphs for which $\Delta H_{\text{trans}}^{298}$ values have been experimentally determined are listed in Table 4 with the respective references. In addition to the molecular sieves, data

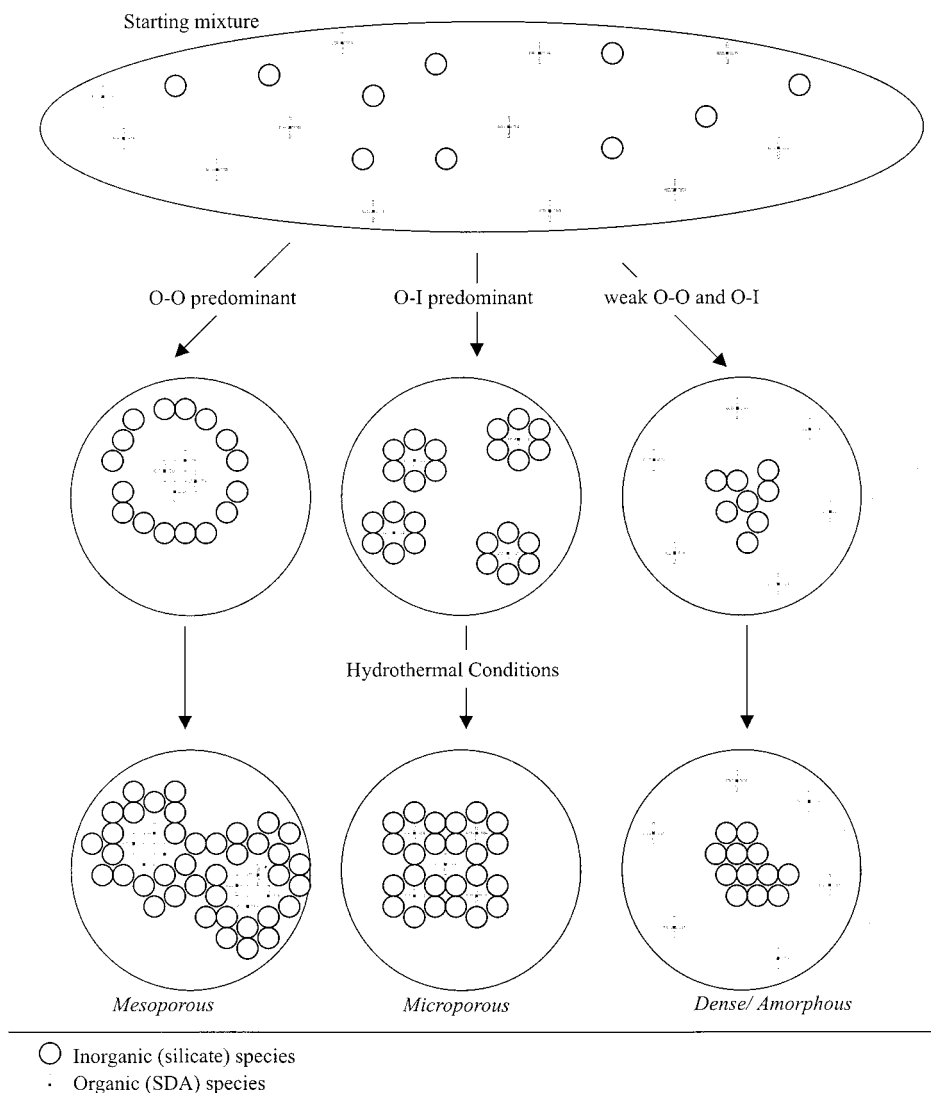


Figure 1. Possibilities for silicate self-assembly in hydrothermal syntheses.

TABLE 4: Relation between Structure and Energetics

sample	framework density (Si/nm ³)	molar volume (cm ³ /mol)	δ (nm)	structure reference	$\Delta H_{\text{trans}}^{298}$ (kJ/mol SiO ₂)	enthalpy reference
quartz	26.52	22.71	0	39	0.0	
MEL	17.80	33.83	0.0496	26	8.2	this work
MWW	16.51	36.47	0.0688	20	10.4	this work
IFR	17.03	35.36	0.0434	17	10.0	this work
ITE	16.26	37.04	0.0617	19	10.1	this work
AST	17.29	34.83	0.0867	12	10.9	this work
STT	16.83	35.78	0.0845	28	9.2	this work
CHA	15.40	39.10	0.0225	16	11.4	this work
BEA	15.60	38.60	N/A	13	9.3	this work
MFI	17.97	33.51	0.0516	27	6.8	this work
CFI	18.28	32.94	0.0376	25	8.8	this work
ISV	15.36	39.21	0.0593	18	14.4	this work
AFI	17.80	33.83	0.0543	40	7.2	8
MTW	19.39	31.06	0.0532	41	8.7	8
FAU	13.45	44.77	0.0242	42	13.6	8
FER	18.43	32.67	0.0494	43	6.6	48
cr	23.37	25.77	0.0127	44	2.84	49
mo	26.22	22.97	0.0379	45	3.4	50
co	29.26	20.58	0.0442	46	2.93	51
tr	22.61	26.63	0.0311	47	3.21	52

for the dense phases cristobalite (cr), tridymite (tr), coesite (co), and moganite (mo) are included. Data for the dense phase stishovite are not included because its Si coordination is not tetrahedral but rather octahedral. The EMT data measured by Petrovic et al.¹ have also been excluded because of the relatively

high (Si/Al = 14.5) Al content. Crystal structures derived from single-crystal studies are available for FER and quartz and must be considered more reliable than those for the other frameworks that were obtained by refinements of powder data (except for MFI, which was not powder but a “twin crystal” with one twin

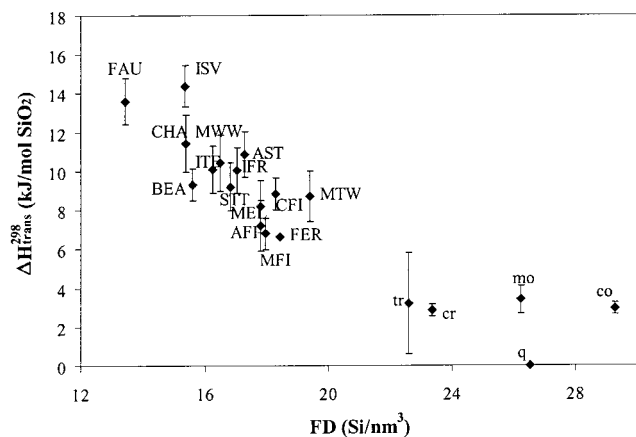


Figure 2. Enthalpy of transition vs framework density.

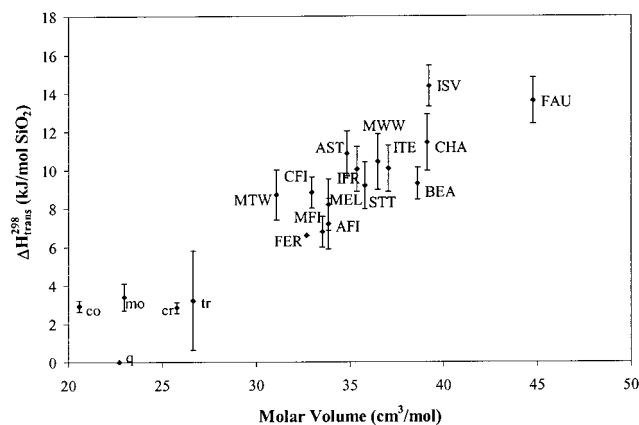


Figure 3. Enthalpy of transition vs molar volume.

much smaller than the other, and the overlapping reflections from both twins were treated mathematically to derive the “true” intensities for the larger twin). This point is relatively unimportant for bulk parameters, such as the framework density and molar volume. The δ parameter discussed below, however, is much more sensitive to atomic configuration, and its precision is affected by uncertainties in the crystal structure accordingly.

Framework Density and Molar Volume. Figures 2 and 3 show the relationship between the $\Delta H_{\text{trans}}^{298}$ values and the FD and molar volume, respectively. The data in Figure 2 clearly exhibit a roughly linear correlation between the $\Delta H_{\text{trans}}^{298}$ values and the framework density for $\text{FD} = 26.55 \text{ Si atoms/nm}^3$ (quartz). Such a trend can be understood in terms of a “quality of packing” argument; in the molecular sieves, the creation of void volumes is possible only with an associated energetic cost corresponding to the inherent instability of the Si atoms that are prevented from collapsing into the void spaces. As the density increases (eliminating void volume), the silica polymorphs become progressively more stable until the most stable structure (quartz) is reached. Further increases in density lead to unfavorable compression, explaining the unstable nature of coesite. The only structure for which the enthalpy differs significantly from the trend above is mo; its relatively high $\Delta H_{\text{trans}}^{298}$ (3.4 kJ/mol) cannot be rationalized on the basis of FD because it has almost exactly the same density as quartz. The enthalpy of moganite was not obtained by a direct measurement but rather by extrapolating measured enthalpies of mo–q intergrowths with varying mo contents to 100% mo.⁵⁰ Hence the reported $\Delta H_{\text{trans}}^{298}$ cannot be considered to be as reliable as those for the other silica polymorphs. Furthermore, the Si–O–Si bonds in mo are more strained than those in q; in particular, four-membered Si

TABLE 5: Measured Enthalpies of Transition vs Predicted Values Based on Molar Volume Correlation

sample	$\Delta H_{\text{trans}}^{298}$ expt (kJ/mol SiO ₂)	$\Delta H_{\text{trans}}^{298}$ predicted (kJ/mol SiO ₂)	error (kJ/mol SiO ₂)
quartz	0	2.4	2.4
MEL	8.2	8.5	0.3
MWW	10.4	9.9	−0.5
IFR	10.0	9.3	−0.7
ITE	10.1	10.2	0.2
AST	10.9	9.0	−1.8
STT	9.2	9.6	0.4
CHA	11.4	11.4	0.0
BEA	9.3	11.1	1.8
MFI	6.8	8.3	1.5
CFI	8.8	8.0	−0.8
ISV	14.4	11.4	−2.9
AFI	7.2	8.5	1.3
MTW	8.7	7.0	−1.7
FAU	13.6	14.5	0.9
FER	6.6	7.8	1.2
cr	2.84	4.0	1.2
mo	3.4	2.5	−0.9
tr	3.21	4.5	1.3
co	2.93	1.2	−1.7

rings are present in mo but not in quartz. Because of the tighter packing, dense silica phases generally have less room for the atoms to rearrange away from the optimal (quartz) configuration than with higher void volumes (molecular sieves). Hence the destabilizing effect of bonding distortions is expected to be the largest for the most dense phases. This observation most likely explains the higher than expected enthalpy of mo and the corresponding departure of the mo data point from the general trend.

The data in Figure 3 show the trends in $\Delta H_{\text{trans}}^{298}$ versus the molar volume of the various silica phases. Because molar volume is inversely proportional to FD, a good correlation is observed between the enthalpies and molar volume. For predictive purposes, a linear regression of the $\Delta H_{\text{trans}}^{298}$ and molar volume data was performed for the phases less dense than quartz, and the results give $\Delta H_{\text{trans}}^{298} = (-10.1 \pm 1.9) + (0.55 \pm 0.06)V_m$, where V_m is the molar volume in cm^3/mol . The molar volume was chosen for the regression rather than the framework density because it allows the regression results to be extended to structures without a regularly repeating framework. Quartz is thermodynamically required to represent a minimum in the enthalpy versus molar volume curve. The coesite data was thus excluded from the correlation because co is a denser yet less stable phase than quartz. Table 5 compares the predicted and experimentally measured $\Delta H_{\text{trans}}^{298}$ values. The calculated value is typically within $<2 \text{ kJ/mol}$ of the experimentally measured $\Delta H_{\text{trans}}^{298}$; that is, the error in the predicted value is only slightly larger than the uncertainty in the measurement itself. Clearly, this empirical correlation is useful to interpolate the enthalpies of transition for other silica phases whose molar volumes are between those of q ($22.71 \text{ cm}^3/\text{mol}$) and FAU ($44.77 \text{ cm}^3/\text{mol}$).

For SiO₂ polymorphs less dense than FAU, the above correlation does not lead one to expect large framework instabilities. Recall that the MCM-41 mesoporous materials (admittedly not crystalline) are much less dense than even the most porous molecular sieve yet have enthalpies of only 14–15 kJ/mol above that of quartz. This observation suggests that the linear molar volume– $\Delta H_{\text{trans}}^{298}$ trend may plateau at high molar volumes (low FD values) as has already been observed for the AlPO₄ materials.³¹ Therefore, very porous materials cannot be sufficiently unstable for their syntheses to be ruled

out based on framework thermodynamics. As pointed out by Davis,⁵³ a purely physical limitation in zeolite syntheses is that the crystal must not float in order for its growth to take place at an appreciable rate in an aqueous system. This restriction does not exclude the formation of frameworks considerably less porous than the ones currently known.⁵³ The difficulty in synthesizing silica polymorphs with $FD \leq FD(\text{FAU})$ so far defies explanation.

Above, the enthalpies have been shown to correlate well with the packing parameters FD and molar volume. These parameters are easy to obtain and are not very sensitive to uncertainties in the crystallographic structure solution. They do not, however, provide significant insight into the nature of the interactions affecting porous silica energetics; in other words, what is the atomic/molecular origin of the destabilization relative to quartz of the silica molecular sieves? To address this issue, we attempted to explore whether other parameters that are based on crystal chemistry concepts would correlate well with the $\Delta H_{\text{trans}}^{298}$ values.

O'Keefe noted that crystallographic evidence shows that for an element in a lattice, such as Si in four-coordinated SiO_2 , there is an optimal Si–Si distance below which electrostatic repulsion becomes excessive.⁵⁴ He therefore suggested correlating framework energetics with nonbonded distances, that is, the distances between nonneighboring atoms. To examine the effect of such nonbonded distances on the framework energetics, we defined a parameter, δ , as the average absolute value of the deviation from the Si–Si distance in quartz (3.0568 Å, calculated from the data in ref 39 and taken as the optimum nonbonded distance for this class of materials):

$$\delta = \frac{\sum_{i=1}^N \sum_{j=1}^4 |d(\text{Si}_i - \text{Si}_j) - 3.0586|}{4N}$$

where $d(\text{Si}_i - \text{Si}_j)$ is the distance from Si atom i to each of its four neighbors j and N is the total number of Si atoms per unit cell. No δ value was calculated for the BEA because its structure is faulted and no single meaningful average nonbonded distance can be defined.

The δ parameter is a *local* measure of the atomic configuration in direct contrast to the *global* description afforded by the framework density FD . An even more local description is given by the loop configuration (defined in the Zeolite Atlas⁸ as a collection of graphs showing how many three- or four-membered rings each type of T atom in a given framework is residing within). The determination here of thermodynamic data for a much more varied collection of silica polymorphs than previously available permitted a conclusive examination of the quality of the correlation between $\Delta H_{\text{trans}}^{298}$ and both of these structural parameters.

Nonbonded Distances. The correlation between $\Delta H_{\text{trans}}^{298}$ and the δ parameter as illustrated by Figure 4 is much weaker than the correlation between $\Delta H_{\text{trans}}^{298}$ and the simple structural parameters FD and molar volume. Although the dense phases that are relatively close in enthalpy to quartz all have low δ values, two of the most unstable silica phases, CHA and FAU, have δ values in the same range (0–0.04 nm). Conversely, the structures with the largest distortions (AST and especially STT) are not the most unstable polymorphs. The structures in the middle δ region ($0.04 \leq \delta \leq 0.08$) show no clear trend either. Rather, the enthalpies appear to plateau at slightly above 10 kJ/mol for high values of δ . This observation is at variance with

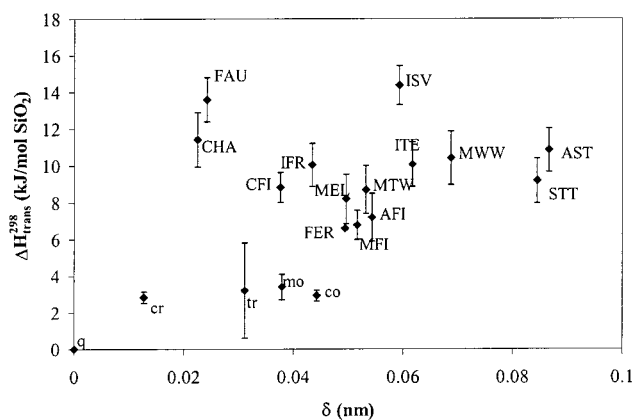


Figure 4. Enthalpy of transition vs δ .

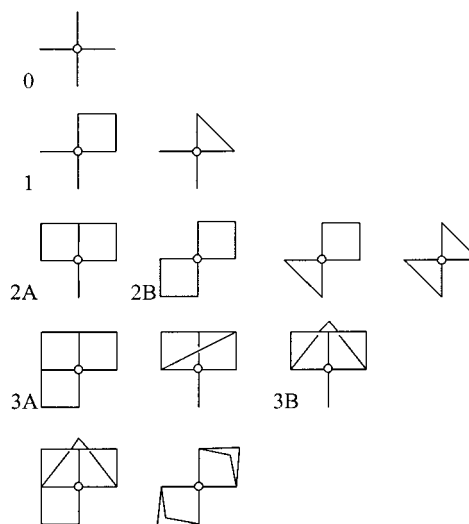


Figure 5. Configuration loops present in zeolites.

the expected physical behavior, namely, the progressive destabilization with increasing δ until the frameworks become so strained that they cannot form under any condition. A comparison between Figures 3 and 4 conclusively shows that the $\Delta H_{\text{trans}}^{298}$ values correlate much better with the molar volume than with δ . Local distortions of the framework, then, do not uniformly determine structural enthalpies; indeed, the large flexibility of T–O–T bonds is traditionally invoked to explain the large number of silica polymorphs that can be synthesized.

Loop Configuration. The loop configuration is a graph representing the number of three- and four-membered rings (3,4-MR) each type of T atom in a framework is residing within. Currently known zeolites and related materials exhibit 12 different types of loop configurations, and they are shown in Figure 5. Calculations predict that 3,4-MR are less stable than six-membered rings (6-MR) by approximately 2.8 (3-MR) and 1.1 (4-MR) kJ/mol.⁵⁵ Five-membered rings, by contrast, are only slightly (0.08 kJ/mol) destabilized relative to 6-MR.⁵⁵ The frameworks whose T atoms are mostly bonded within multiple 3,4-MR, then, are expected to be less stable than structures devoid of them. Table 6 lists the fractions, f , of T atoms engaged in the various loop configuration types for each silica phase for which enthalpy data are available. Six of the 12 possible loops are represented, and the frameworks contain from 0% 3,4-MR (q, tr, cr, and FER) up to 100% loops containing three 4-MR (CHA, FAU). Unfortunately, no pure- SiO_2 material with 3-MR has yet been prepared by direct synthesis, so only the effect of 4-MR will be examined here. The molecular sieves that consist mostly ($f_0 + f_1 \geq 75\%$) of zero or only one 4-MR (AFI, MTW,

TABLE 6: Fractional Contributions of Loop Configuration Types to Silica Structures

structure	loop type					
	0 0 ring	1 1 ring	2A 2 rings	2B 2 rings	3A 3 rings	3B 3 rings
AFI	0.00	1.00	0.00	0.00	0.00	0.00
AST	0.20	0.00	0.00	0.00	0.00	0.80
BEA	0.25	0.25	0.50	0.00	0.00	0.00
CHA	0.00	0.00	0.00	0.00	1.00	0.00
MTW	0.71	0.29	0.00	0.00	0.00	0.00
MFI	0.83	0.17	0.00	0.00	0.00	0.00
MEL	0.58	0.42	0.00	0.00	0.00	0.00
FAU	0.00	0.00	0.00	0.00	1.00	0.00
MWW	0.22	0.50	0.17	0.00	0.00	0.11
FER	1.00	0.00	0.00	0.00	0.00	0.00
CFI	0.75	0.00	0.25	0.00	0.00	0.00
IFR	0.00	0.25	0.50	0.25	0.00	0.00
ITE	0.00	0.25	0.50	0.25	0.00	0.00
STT	0.13	0.31	0.38	0.13	0.06	0.00
ISV	0.25	0.25	0.00	0.00	0.00	0.50
quartz	1.00	0.00	0.00	0.00	0.00	0.00
tr	1.00	0.00	0.00	0.00	0.00	0.00
cr	1.00	0.00	0.00	0.00	0.00	0.00
co	0.00	0.00	1.00	0.00	0.00	0.00
mo	0.00	0.67	0.00	0.33	0.00	0.00

TABLE 7: Enthalpy Contributions for Loop Types

loop type	contribution (kJ/mol)		loop type	contribution (kJ/mol)	
	enthalpy	std error		enthalpy	std error
0	4.9	1.3	2B	-0.5	7.8
1	4.5	3.1	3A	7.6	2.6
2A	3.0	3.0	3B	10.2	3.8

MFI, MEL, FER, and CFI are the most stable frameworks; they all have $\Delta H_{\text{trans}}^{298} \leq 8.8$ kJ/mol. Conversely, the structures that contain mainly ($f_{3A} + f_{3B} \geq 50\%$) triple 4-MR (CHA, ISV, FAU, and AST) are the least stable frameworks, with $\Delta H_{\text{trans}}^{298} \geq 10.8$ kJ/mol. The presence of large fractions of multiple 4-MR, then, seems to lead to a destabilization of the framework. When the dense phases are examined as well, however, the trend becomes less evident: q, tr, and cr have the same loop configuration as FER yet are up to 6.6 kJ/mol more stable. Further, coesite consists solely of loops containing two 4-MR, yet it is only 2.9 kJ/mol less stable than quartz.

To evaluate these data more quantitatively, a linear regression was performed to fit the enthalpy data to the distribution of loop types, according to

$$\Delta H_j = e_0 + \sum_{i \neq 0} e_i f_{ij}$$

where f_{ij} is the fraction of loop type i present in structure j and e_i is the energetic contribution of loop type i (to be determined). Because only 20 data points are available to determine 5 parameters, the results must be interpreted with caution; Table 7 lists the e_i coefficients with their associated standard errors, and Table 8 compares the calculated enthalpy from this relation, ΔH_j , to the measured $\Delta H_{\text{trans}}^{298}$. A comparison between the data in Tables 5 and 8 clearly shows that the correlation based on molar volume is much more accurate in its $\Delta H_{\text{trans}}^{298}$ predictions than the loop configuration correlation, despite the much larger number of independent variables in the latter. In particular, the loop configuration correlation severely overestimates the enthalpies of transition of the dense phases. This systematic error is due to the fact that the loop descriptions for the most stable molecular sieves and the dense phases q, tr, and cr are quite similar ($f_0 > 0.70$), even though there are significant enthalpy differences between the two groups.

TABLE 8: Measured Enthalpies of Transition vs Predicted Values Based on Loop Configuration Correlation

structure	$\Delta H_{\text{trans}}^{298}$ expt (kJ/mol SiO ₂)	ΔH_j (fit) (kJ/mol SiO ₂)	error (kJ/mol SiO ₂)
AFI	7.2	9.5	2.3
AST	10.9	13.1	2.2
BEA	9.3	7.6	-1.7
CHA	11.4	12.5	1.1
MTW	8.7	6.2	-2.5
MFI	6.8	5.7	-1.1
MEL	8.2	6.8	-1.4
FAU	13.6	12.5	-1.1
MWW	10.4	8.8	-1.6
FER	6.6	4.9	-1.7
CFI	8.8	5.7	-3.1
IFR	10.0	7.5	-2.6
ITE	10.1	7.5	-2.6
STT	9.2	7.9	-1.3
ISV	14.4	11.2	-3.2
q	0	4.9	4.9
tr	3.2	4.9	1.7
cr	2.8	4.9	2.1
co	2.9	7.9	5.0
mo	3.4	7.8	4.4

In summary, the data presented here for low-FD, directly synthesized SiO₂ phases show that $\Delta H_{\text{trans}}^{298}$ correlates well with the molar volume (or, equivalently, the FD) of SiO₂ polymorphs. This correlation expresses the effect of the overall quality of packing on the framework enthalpies. The new data conclusively discredit any correlation between $\Delta H_{\text{trans}}^{298}$ and the nonbonded parameter δ . Although large fractions of Si atoms involved in 4-MR result in less stable structures, the quantitative correlation between $\Delta H_{\text{trans}}^{298}$ and loop configuration is not very good. This is especially true for the dense phases for which the enthalpies of the 4-MR-containing phases coe and mo are severely overestimated. Finally, the enthalpies for the large number of high-quality SiO₂ polymorphs reported here conclusively show that the class of crystalline SiO₂ materials lies within a narrow range and is not dramatically destabilized from quartz.

Conclusions

The enthalpies of transition for a series of pure-SiO₂ molecular sieves with varied structural features (low density, large rings) have been determined by drop solution calorimetry in lead borate at 974 K. All samples in this study have enthalpies that fall in a narrow range of 6.8–14.4 kJ/mol less stable than that of quartz and are in excellent agreement with previously reported values. This range (7.6 kJ/mol) is comparable to twice the available thermal energy (6.2 kJ/mol) at typical synthesis conditions. All known tetrahedrally coordinated SiO₂ polymorphs, then, are only slightly metastable with respect to quartz. This low barrier to transformation explains the large diversity (around 30 structures) of SiO₂ polymorphs. Furthermore, the role of the organic structure-directing agents used in zeolite synthesis cannot be the stabilization of otherwise very unstable structures. They may, however, stabilize one structure at the expense of others by forming inorganic–organic composites.

The pure-SiO₂ molecular sieve enthalpies correlate well with molar volume and framework density but rather poorly with nonbonded Si–Si distances and loop configuration. The overall quality of packing of the SiO₄ tetrahedra is thus the most important parameter affecting the framework stability. Finally, the presence of silanol defect groups has been shown to slightly raise the enthalpies of transition relative to quartz when compared to the low-defect density frameworks.

Acknowledgment. Financial support for this work was provided by the Chevron Research and Technology Company. The calorimetric studies were supported by National Science Foundation Grant DMR 97-31782. P.M.P. thanks Katsuyuki Tsuji for providing one of the samples used in this study and Michael Gordon (Caltech) for helping in the design of sample transfer vessels. Comments by Dr. Stacey I. Zones (Chevron) are appreciated.

References and Notes

- (1) Petrovic, I.; Navrotsky, A.; Davis, M. E.; Zones, S. I. *Chem. Mater.* **1993**, *5*, 1805.
- (2) Navrotsky, A. *MRS Bull.* **1995**, May, 35.
- (3) Breck, D. W. *Zeolite Molecular Sieves*; Wiley: New York, 1974.
- (4) Gies, H.; Marler, B. *Zeolites* **1992**, *12*, 42.
- (5) Lobo, R. F.; Zones, S. I.; Davis, M. E. *J. Inclusion Phenom. Mol. Recognit. Chem.* **1995**, *21*, 47.
- (6) Davis, M. E.; Zones, S. I. In *Synthesis of Porous Materials*; Occelli, M. L., Kessler, H., Eds.; Marcel Dekker: New York, 1997.
- (7) Helmkamp, M. M.; Davis, M. E. *Annu. Rev. Mater. Sci.* **1995**, *25*, 161.
- (8) See: <http://www.iza-sc.ethz.ch/IZA-SC/Atlas/AtlasHome.html>.
- (9) Henson, N. J.; Cheetham, A. K.; Gale, J. D. *Chem. Mater.* **1994**, *6*, 1647.
- (10) Cambor, M. A.; Villaescusa, L. A.; Díaz-Cabañas, M.-J. *Top. Catal.* **1999**, *9*, 59.
- (11) Ohsuna, T.; Terasaki, O.; Nakagawa, Y.; Zones, S. I.; Hiraga, K. *J. Phys. Chem. B* **1997**, *101*, 9881.
- (12) Villaescusa, L. A.; Barrett, P. A.; Cambor, M. A. *Chem. Mater.* **1998**, *10*, 3966.
- (13) Cambor, M. A.; Corma, A.; Valencia, S. *Chem. Commun.* **1996**, 2365.
- (14) Tsuji, K.; Beck, L. W.; Davis, M. E. *Microporous Mesoporous Mater.* **1999**, *28*, 519.
- (15) Barrett, P. A.; Díaz-Cabañas, M.-J.; Cambor, M. A.; Jones, R. H. *J. Chem. Soc., Faraday Trans.* **1998**, *94*, 2475.
- (16) Díaz-Cabañas, M.-J.; Barrett, P. A.; Cambor, M. A. *Chem. Commun.* **1998**, 1881.
- (17) Barrett, P. A.; Cambor, M. A.; Corma, A.; Jones, R. H.; Villaescusa, L. A. *Chem. Mater.* **1997**, *9*, 1713.
- (18) Villaescusa, L. A.; Barrett, P. A.; Cambor, M. A. *Angew. Chem., Int. Ed. Engl.* **1999**, *38*, 1997.
- (19) Cambor, M. A.; Corma, A.; Lightfoot, P.; Villaescusa, L. A.; Wright, P. A. *Angew. Chem., Int. Ed. Engl.* **1997**, *36*, 2659.
- (20) Cambor, M. A.; Corma, A.; Díaz-Cabañas, M.-J.; Baerlocher, Ch. *J. Phys. Chem. B* **1998**, *102*, 44.
- (21) Cambor, M. A.; Díaz-Cabañas, M.-J.; Perez-Pariente, J.; Teat, S. J.; Clegg, W.; Shannon, I. J.; Lightfoot, P.; Wright, P. A.; Morris, R. E. *Angew. Chem., Int. Ed. Engl.* **1998**, *37*, 2122.
- (22) Navrotsky, A. *Phys. Chem. Miner.* **1977**, *2*, 89.
- (23) Navrotsky, A. *Phys. Chem. Miner.* **1997**, *24*, 3.
- (24) Navrotsky, A.; Rapp, R. P.; Smelik, E.; Burnley, P.; Circone, S.; Chai, L.; Bose, K. *Am. Mineral.* **1994**, *79*, 1099.
- (25) Yoshikawa, M.; Wagner, P.; Lovallo, M.; Tsuji, K.; Takewaki, T.; Chen, C.-Y.; Beck, L. W.; Jones, C.; Tsapatsis, M.; Zones, S. I.; Davis, M. E. *J. Phys. Chem. B* **1998**, *102*, 7139.
- (26) Terasaki, O.; Ohsuna, T.; Sakuma, H.; Watanabe, D.; Nakagawa, Y.; Medrud, R. C. *Chem. Mater.* **1996**, *8*, 463.
- (27) van Koningveld, H.; Jansen, J. C.; van Bekkum, H. *Zeolites* **1990**, *10*, 235.
- (28) Cambor, M. A.; Díaz-Cabañas, M.-J.; Cox, P. A.; Shannon, I. J.; Wright, P. A.; Morris, R. E. *Chem. Mater.* **1999**, *11*, 2878.
- (29) Nakagawa, Y.; Lee, G. S.; Harris, T. V.; Yuen, L. T.; Zones, S. I. *Microporous Mesoporous Mater.* **1998**, *22*, 69.
- (30) Robie, R. A.; Hemingway, B. S. *Thermodynamic properties of minerals and related substances at 298.15 K and 1 bar pressure and at higher temperatures*; USGS Bulletin 2131; U.S. Geological Survey: Reston, VA, 1995.
- (31) Hu, Y.; Navrotsky, A.; Chen, C.-Y.; Davis, M. E. *Chem. Mater.* **1995**, *7*, 1816.
- (32) Blasco, T.; Cambor, M. A.; Corma, A.; Esteve, P.; Guil, J. M.; Martínez, A.; Perdígón-Melón, J. A.; Valencia, S. *J. Phys. Chem. B* **1998**, *102*, 75.
- (33) Kiseleva, I.; Navrotsky, A.; Belitsky, I. A.; Fursenko, B. A. *Am. Mineral.* **1996**, *81*, 658.
- (34) Gale, J. D. *GULP (the General Utility Lattice Program)*; Royal Institution/Imperial College: U.K., 1992–1994.
- (35) Maniar, P. D.; Navrotsky, A.; Rabinovich, E. M.; Ying, J. Y.; Benziger, J. B. *J. Non-Cryst. Solids* **1990**, *124*, 101.
- (36) Ying, J. Y.; Benziger, J. B.; Navrotsky, A. *J. Am. Ceram. Soc.* **1993**, *76*, 257.
- (37) Petrovic, I.; Navrotsky, A.; Chen, C.-Y.; Davis, M. E. *Stud. Surf. Sci. Catal.* **1994**, *84*, 677.
- (38) Newton, M. D.; Gibbs, G. V. *Phys. Chem. Miner.* **1980**, *6*, 221.
- (39) Levien, L.; Prewitt, C. T.; Weidner, D. J. *Am. Mineral.* **1980**, *65*, 920.
- (40) Bialek, R.; Meier, W. M.; Davis, M.; Annen, M. J. *Zeolites* **1991**, *11*, 438.
- (41) Fyfe, C. A.; Gies, H.; Kokotailo, G. T.; Marler, B.; Cox, D. E. *J. Phys. Chem.* **1990**, *94*, 3718.
- (42) Hriljac, J. A.; Eddy, M. M.; Cheetham, A. K.; Donohue, J. A.; Ray, G. J. *J. Solid State Chem.* **1993**, *106*, 66.
- (43) Lewis, J. E., Jr.; Freyhardt, C. C.; Davis, M. E. *J. Phys. Chem.* **1996**, *100*, 5039.
- (44) Pluth, J. J.; Smith, J. V.; Faber, J. J., Jr. *Appl. Phys.* **1985**, *57*, 1045.
- (45) Miehle, G.; Graetsch, H. *Eur. J. Mineral.* **1992**, *4*, 693.
- (46) Smyth, J. R.; Smith, J. V.; Artioli, G.; Kvik, A. *J. Phys. Chem.* **1987**, *91*, 988.
- (47) Dollase, W. A.; Baur, W. H. *Am. Mineral.* **1976**, *61*, 971.
- (48) Petrovic, I.; Navrotsky, A. Unpublished results.
- (49) Richet, P.; Bottinga, Y.; Denielou, L.; Petitet, J. P.; Tequi, C. *Geochim. Cosmochim. Acta* **1982**, *46*, 2639.
- (50) Petrovic, I.; Heaney, P. J.; Navrotsky, A. *Phys. Chem. Miner.* **1996**, *23*, 119.
- (51) Akaogi, M.; Navrotsky, A. *Phys. Earth Planet. Inter.* **1984**, *36*, 124.
- (52) Robie, R. A.; Hemingway, B. S.; Fisher, J. R. *Thermodynamic properties of minerals and related substances at 298.15 K and 1 bar pressure and at higher temperatures*; USGS Bulletin 1452; U.S. Geological Survey: Reston, VA, 1978.
- (53) Davis, M. E. *Chem.—Eur. J.* **1997**, *3*, 1745.
- (54) O'Keefe, M.; Hyde, B. G. In *Structure and Bonding in Crystals*; O'Keefe, M., Navrotsky, A., Eds.; Academic Press: New York, 1981.
- (55) Gibbs, G. V. Personal communication, 1998.